THE SYMMETRY OF VESUVIANITE

LEE A. GROAT

Department of Geological Sciences, University of British Columbia, Vancouver, British Columbia V6T 1Z4

FRANK C. HAWTHORNE

Department of Geological Sciences, University of Manitoba, Winnipeg, Manitoba R3T 2N2

T. SCOTT ERCIT

Mineral Sciences Section, Canadian Museum of Nature, Ottawa, Ontario K1P 6P4

ANDREW PUTNIS

Department of Earth Sciences, University of Cambridge, Cambridge CB2 3EQ, England

ABSTRACT

The vesuvianite structure has ideal symmetry $P4/nnc$, but many vesuvianite samples show physical properties that indicate deviations from this symmetry. Here we examine 76 samples of vesuvianite from approximately 50 different localities, and focus on their physical and chemical properties that are affected by symmetry. Three groups are recognized, on the basis of optical properties: (i) normal crystals of vesuvianite show uniform extinction and small (0–5°) $2V$; (ii) blocky crystals of vesuvianite show irregularly shaped areas of variable birefringence in a (001) section, with $2V$ values in the range 5–35°; (iii) sector-zoned crystals of vesuvianite show {001}, {101} and {100} sectors with low (~5°), intermediate (20–35°) and high (40–60°) values of $2V$, respectively; some crystals may be more complex, with {110} zones. X-ray precession photographs of fragments from each of the sectors show the number and intensity of the "glide-violating" reflections to increase in the sequence {101} → {001} → {100}; in addition, deviations from $4/mmm$ Laue symmetry also were apparent. Diffuse streaking is associated with the "violating" reflections. Possible derivative space-groups can be derived from the $P4/nnc$ parent group using group-reduction techniques. This shows that several space groups previously suggested are not possible. In addition, several of the derivative space-groups can be eliminated, as the observed optic orientations are not compatible with these symmetries. A combination of optical and X-ray-diffraction evidence indicates that the symmetry of vesuvianite is $P2/n$ (or Pn). We suggest that there is a continuous (or near-continuous) ferroelastic phase transition between a high-temperature $P4/nnc$ structure and a low-temperature $P2/n$ or Pn structure. Differential order of cations over pairs of sites in the channels of the structure cannot drive the transition to $P2/n$ symmetry, as the associated order-parameter does not transform as the active irreducible representation of this transition. The variety of optical types of vesuvianite are a result of different relationships between the temperature interval of crystallization and the temperature of the phase transition.

Keywords: vesuvianite, symmetry, ferroelastic phase transition, channel, degree of order.

SOMMAIRE

La structure de la vésuvianite possède une symétrie idéale $P4/nnc$, mais les propriétés physiques de plusieurs échantillons témoignent d'une symétrie différente. Nous examinons ici soixante-seize échantillons provenant de cinquante localités différentes, en portant notre attention sur les propriétés physiques et chimiques qui sont affectées par la symétrie. Nous répartissons les échantillons en trois groupes selon leurs propriétés optiques: i) cristaux normaux montrant un angle d'extinction uniforme et un angle $2V$ faible (0–5°); ii) cristaux en blocs montrant des zones à forme irrégulière, de biréfringence variable dans une section (001), avec $2V$ entre 5 et 35°, et iii) cristaux à zonation en secteurs, ayant des secteurs {001}, {101} et {100} avec $2V$ faible (~5°), intermédiaire (20–35°), et élevé (40–60°), respectivement. Certains de ces cristaux seraient même plus complexes, et montrent des zones {110}. D'après les clichés de précession (en diffraction X) de fragments provenant de chacun de ces secteurs, le nombre et l'intensité des réflexions en violation des plans de glissement augmentent dans l'ordre {101} → {001} → {100}. De plus, les écarts à la symétrie de Laue $4/mmm$ sont évidents. L'étirement des taches est lié à la présence de réflexions qui causent les violations. Les groupes spatiaux dérivatifs possibles découlent du groupe parent $P4/nnc$ par techniques de réduction de groupe. Plusieurs groupes spatiaux proposés antérieurement ne sont pas des choix possibles. De plus, plusieurs des groupes spatiaux dérivatifs peuvent être éliminés à cause de leur incompatibilité avec les orientations optiques observées. Une combinaison des évidences optiques et en diffraction X montre que la symétrie de la vésuvianite serait $P2/n$ (ou Pn). Nous croyons qu'il existe une transition ferroélastique continue (ou presque) entre une structure $P4/nnc$ stable à température élevée et une structure $P2/n$ ou Pn stable à faible température. Une mise en ordre différentielle des cations impliquant des paires de

sites dans les canaux de la structure ne saurait être responsable d'une transition à la symétrie $P2/n$, parce que le paramètre de mise en ordre associé ne se transforme pas dans la représentation active irréductible de cette transition. La variété des types optiques de la vésuvianite résulte des relations entre l'intervalle de température de cristallisation et la température de l'inversion.

(Traduit par la Rédaction)

Mots-clés: vésuvianite, symétrie, transition de phase ferro-élastique, canal, degré d'ordre.

INTRODUCTION

Vesuvianite is a common rock-forming and accessory silicate mineral. In most texts on mineralogy and optical mineralogy, it is described as tetragonal, with the occasional comment that optically anomalous and biaxial varieties also are known. In fact, there are major uncertainties in the symmetry, structure and chemistry of vesuvianite, uncertainties that have resisted considerable effort to clarify and understand them. As part of a general investigation of vesuvianite (Groat *et al.* 1992a, b), we here examine the structural and physical characteristics that pertain to the question of symmetry and the factors that affect it.

PREVIOUS WORK

There are two principal types of experimental information that have been used in the derivation of the symmetry of vesuvianite: optics and diffraction. We will review the published work in some detail, as it indicates some of the ways in which the problem can be approached from new directions.

Optical evidence

Vesuvianite commonly occurs as very large and well-developed euhedral crystals that exhibit tetragonal morphology. Nevertheless, examination in transmitted light shows them commonly to be biaxial, and some show complex sector-zoning. These features were discussed in detail by Arem (1973), and it is apparent from his review that vesuvianite shows an extremely wide variation in optical properties: "no two idocrase specimens seemed to give the same results". Important optical features of vesuvianite are summarized as follows: (i) Some vesuvianite samples are uniaxial. (ii) Many vesuvianite samples are biaxial, with $2V$ varying in the range 0–62°. (iii) Some vesuvianite crystals are sector-zoned, the sectors being related to the bounding crystal faces. The sectors are subtended by a specific face at the surface of the crystal, and sectors may be identified by the Miller indices of the subtending face (or form). (iv) Some vesuvianite crystals show an irregular zonal pattern (if cut normal to the Z axis), with the different zones extinguishing in different positions; these crystals show

complete homogeneity in all major elements (Ca, Si, Al, Mg, Fe) (Arem 1973). (v) Some vesuvianite crystals show a lamellar structure that, in Arem's opinion, is due to twinning.

Much work has been published on the optical properties of vesuvianite, and there is sufficient reproducibility from locality to locality as studied by different investigators to indicate that the differences in optical properties are real.

Diffraction evidence

Warren & Modell (1931) solved the crystal structure of vesuvianite in the space-group $P4/nnc$. This symmetry was assumed to be correct until the work of Arem & Burnham (1969). Using precession photography, these authors showed that one or more of the glide-plane extinction criteria for $P4/nnc$ symmetry are violated in many samples from a variety of localities; thus a variety of space-groups were proposed (Table 1). Vesuvianite samples from several localities have $P4/nnc$ symmetry; for some other localities, the symmetry is reduced. The space-group $P4/nmm$ was proposed, with the deviations from $P4/nnc$ symmetry characterized as "strong" and "weak". Violations of the n-glide perpendicular to [001] also were observed in three samples, giving the possible space-groups $P4/mmm$, $P\bar{4}2m$, $P\bar{4}m2$, $P4mm$ and $P422$; for one sample from Asbestos, Quebec, a positive piezoelectric response eliminated $P4/mmm$ as a possibility

TABLE 1. NON-$P4/nnc$ SPACE GROUPS REPORTED IN PREVIOUS STUDIES

Space Group	Locality	Study
$P4/nmm$ - "strong"	Black Lake, Que.	Arem & Burnham (1969)
"	Coleraine, Que.	"
"	Laurel, Que.	"
"	Eden Mills, VT	"
$P4/nmm$ - "weak"	Monte Somma, Italy	"
"	Telemark, Norway	"
"	Franklin, NJ	"
$4/mmm$ - P-/---	Asbestos, Que.	"
"	Hindubagh, Pakistan	"
"	San Benito Co., CA	"
$P4/mmm$	Polyanthos, Greece	Sapountzis & Katagas (1980)
$P4/n$	Ala Piedmont, Italy	Giuseppetti & Mazzi (1983)
"	Asbestos, Que.	Allen & Burnham (1983a, b)
"	Eden Mills, VT	"
$P\bar{4}$	Eden Mills, VT	Allen (1985)
$P4/n$	Asbestos, Que.	Fitzgerald *et al.* (1986b)
"	San Benito Co., CA	Fitzgerald *et al.* (1987)

	P4/n		P4nc	
	OR		OR	
O(10)A Y(1)A	O(10)A X(4)B	O(10)A X(4)B	O(10)A Y(1)A
O(10)B X(4)A	O(10)B Y(1)B	O(10)B Y(1)B	O(10)B X(4)A
X(4)A O(10)B	Y(1)B O(10)B	X(4)A O(10)B	Y(1)B O(10)E
Y(1)A O(10)A	X(4)B O(10)A	Y(1)A O(10)A	X(4)B O(10)A
A	B	C	D

FIG. 1. Possibilities for order among channel cations in the vesuvianite structure; arrangements A and B are compatible with P4/n symmetry, C and D are compatible with P4nc symmetry, and a statistical combination of all four arrangements is compatible with P4/nnc symmetry. The notation of sites is from Groat et al. (1992a).

(although the ubiquity of quartz as inclusions in vesuvianite makes this a very difficult experiment).

Sapountzis & Katagas (1980) assigned the space-group P4/nnm to a vesuvianite sample from Greece. Allen (1985) suggested a further set of non-tetragonal space-groups (Table 1) as possible symmetries for vesuvianite, based on the fact that many samples are biaxial rather than uniaxial as required by tetragonal symmetry.

Giuseppetti & Mazzi (1983) were the first to attack the problem of non-P4/nnc vesuvianite, refining the structure of a vesuvianite crystal from Val d'Ala, Piemonte, in the space-group P4/n. This particular crystal showed large numbers of weakly observed reflections of the type h0l, h + k odd, and hhl, l odd, consistent with the space-group P4/n. This reduction in symmetry allows additional ordering of the cations that occupy the channel sites in the structure. The possibilities for such ordering are shown in Figure 1; arrangements A and B are compatible with P4/n symmetry, arrangements C and D are compatible with P4nc symmetry, and a statistical combination of all four arrangements is compatible with P4/nnc symmetry. For P4/n symmetry, each channel site equivalent in P4/nnc is split into two nonequivalent sites of similar geometry. Site-occupancy refinements by Giuseppetti & Mazzi (1983) showed that there is significant ordering over the pseudo-equivalent sites in the channel. More recent refinements in P4/n and P4 were reported by Allen (1985), Allen & Burnham (1983a, b) and Fitzgerald et al. (1986, 1987), and various discussions of possible schemes of order compatible with different tetragonal symmetries have been given. Allen & Burnham (1992) have further developed the scheme of Giuseppetti & Mazzi (1983). They proposed that vesuvianite consists of ordered domains based on P4/n, P4, P4nc or lower symmetry. Crystals with equal volumes of domains show P4/nnc (long-range) symmetry, whereas crystals with unequal volumes of (differently ordered) domains show symmetry "consistent with the preferred scheme of order".

The proposed differences in the various domains are associated with different schemes of order at the partly occupied Y(1) and X(4) sites in the channels of the structure. These and previous arguments have not specifically addressed the non-tetragonal aspects of the vesuvianite structure; this is done here.

EXPERIMENTAL

Groat et al. (1992a) characterized the chemistry of a wide range of vesuvianite samples that form the basis for the work presented here. Selected samples from this set are examined by optical methods, precession photography, single-crystal X-ray diffractometry and high-resolution transmission electron microscopy (HRTEM).

Optics

Sections were prepared both parallel to (001) and (100), generally 250 μm in thickness. For most of the samples listed by Groat et al. (1992a), 2V was measured by the method of Tobi or Kamb (Bloss 1961). To check on the reliability of these measurements, 2V also was measured on a spindle stage with a filtered source (λ = 590 nm), using the program EXCALIBR (Bloss 1981). For crystals in which sector zoning was observed, serial sections were cut such that the three-dimensional nature of the sector zoning could be recorded.

Some simple heating experiments were done with a Fluid, Inc. fluid-inclusion heating stage on a Nikon Optiphot microscope. A (001) section of sample V12 was heated in air from 25 to 500°C and simultaneously examined in cross-polarized light to observe the effect of temperature on the deviation from uniaxial optics.

Precession photography

Following detailed electron-microprobe analysis of oriented sections, specific fragments of the crystal were removed from the thick section for precession photography; in this way, the chemistry and optical properties of the fragment were known prior to the diffraction experiment. In addition, this enabled spindle-stage measurements of 2V to be compared with analogous values obtained by the Tobi or Kamb methods. These fragments were ground into spheres to eliminate differential absorption as a function of crystal orientation, as this can be a source of apparent deviations in diffraction intensities from the true (Laue) symmetry of the crystal.

These crystals were mounted on glass fibers and examined on a conventional precession camera with filtered MoKα X-radiation. Long-exposure zero- and upper-level precession photographs were taken with "wet" film. All photographs were taken at two differ-

ent values of the precession angle (usually 25° and 30°) in order to identify possible Renninger (double-diffraction) effects.

Cell dimensions

Groat *et al.* (1992a) measured cell dimensions on all their chemically characterized samples using single-crystal X-ray diffractometry. However, they constrained their cell dimensions to tetragonal symmetry ($a = b$). We rerefined these data without any metric constraints on the cell dimensions so that the refinement results are free to reflect any metric deviations of the unit cell from tetragonal symmetry.

Measurement of diffraction intensities

Crystals were mounted on a Nicolet *R3m* automated four-circle diffractometer equipped with a molybdenum X-ray tube and a highly oriented graphite-crystal monochromator mounted in equatorial geometry. Twenty-five reflections were automatically centered, and least-squares refinement produced the cell dimensions (Table 2) and an orientation matrix relating the crystal axes to the diffractometer axes. Intensity data were collected in $\theta - 2\theta$ scan mode according to the procedure of Groat *et al.* (1992b). Complete sets of selected equivalent reflections (in 4/*mmm* Laue symmetry) were collected in order to quantitatively compare the intensity distributions with the possible Laue elements of symmetry. Intensities systematically absent in *P4/nnc* symmetry also were collected.

High-resolution transmission electron microscopy

A (100) section of V12 was examined with an Hitachi 100 kV transmission electron microscope, equipped with a tilting stage. An ion mill was used to make an edge thin enough to allow transmission of the electron beam. Both HRTEM images and selected-area diffraction (SAD) patterns were obtained from the sample.

TABLE 3. OPTICAL FEATURES OF SELECTED VESUVIANITE CRYSTALS

Sample	Locality	2V (°)*
	Blocky Zoning	
V4	Turnback Lake, N.W.T.	7 (core), 8-19 (rim)
V10	Jeffrey Mine, Que.	9-24 (core), 32.8(4) (rim)
V11	"	30-33 (core), 37-40 (rim)
V15	"	39
V16	"	
V20	"	62.1(3)
V21	"	
V22	"	13-21 (core), 44.7(2) (rim)
V31	Wakefield Township, Que.	0-10 (core), 14-23 (rim)
V49	Hindubagh, Pakistan	
	Sector Zoning	
V7	Black Lake, Que.	6-9
V12	Jeffrey Mine, Que.	0-10 (core), 36 ({101}), 60-62 (rim)
V44	Laguna del Jaco, Mexico	
V72	Eden Mills, VT	
V75	Wilui River, U.S.S.R.	0-10 (core), 10-25 ({101} and rim)

*The values with standard deviations were obtained with a spindle stage. All others except V12 (rim; Tobi's Method) were determined using Kamb's Method (Bloss 1961).

RESULTS

Optics

2V measurements. Variations in birefringence are a prominent feature of some samples of vesuvianite; we describe these variations with the terms "low", "intermediate" and "high", emphasizing that high birefringence is of the order 0.003. Values of *2V* for selected samples are given in Table 3; values vary from 0 to over 60°. It should be noted that where *2V* is small (<5°), the isogyres tend to be rather diffuse, and it is difficult to differentiate between true uniaxial behavior and slight biaxiality. There is good agreement between the spindle-stage and thin-section measurements of *2V*, indicating that the latter are reasonably accurate (perhaps ±2°). All samples of boron-free vesuvianite are optically negative; all boron-bearing samples are optically positive. This confirms the observations of Oftedal (1964), Khotina (1968) and Serdyuchenko *et al.* (1968). At boron contents somewhat less than the minimum (1.25 atoms per formula unit) found by Groat *et al.* (1992a) in crystals of boron-bearing vesuvianite, there must be an isotropic vesuvianite (assuming complete solid-solution between boron-free and boron-bearing vesuvianites).

Textural types. The vesuvianite samples examined in thin (thick) section show a variety of textures in both plane- and cross-polarized light. They can be divided into three basic types: (i) *Normal vesuvianite:* these crystals show uniform extinction and usually have a small *2V*; the majority (~95%) of vesuvianite samples are of this type. An example is shown in Figure 2a (V40, Monte Somma, Italy). Although there is uniform extinction, a pronounced optical zoning is present. A BSE image (Fig. 2b) shows the optical zoning to correspond to differences in mean atomic number. (ii) *Blocky vesuvianite:* the (001) section is divided into irregularly shaped areas of variable bire-
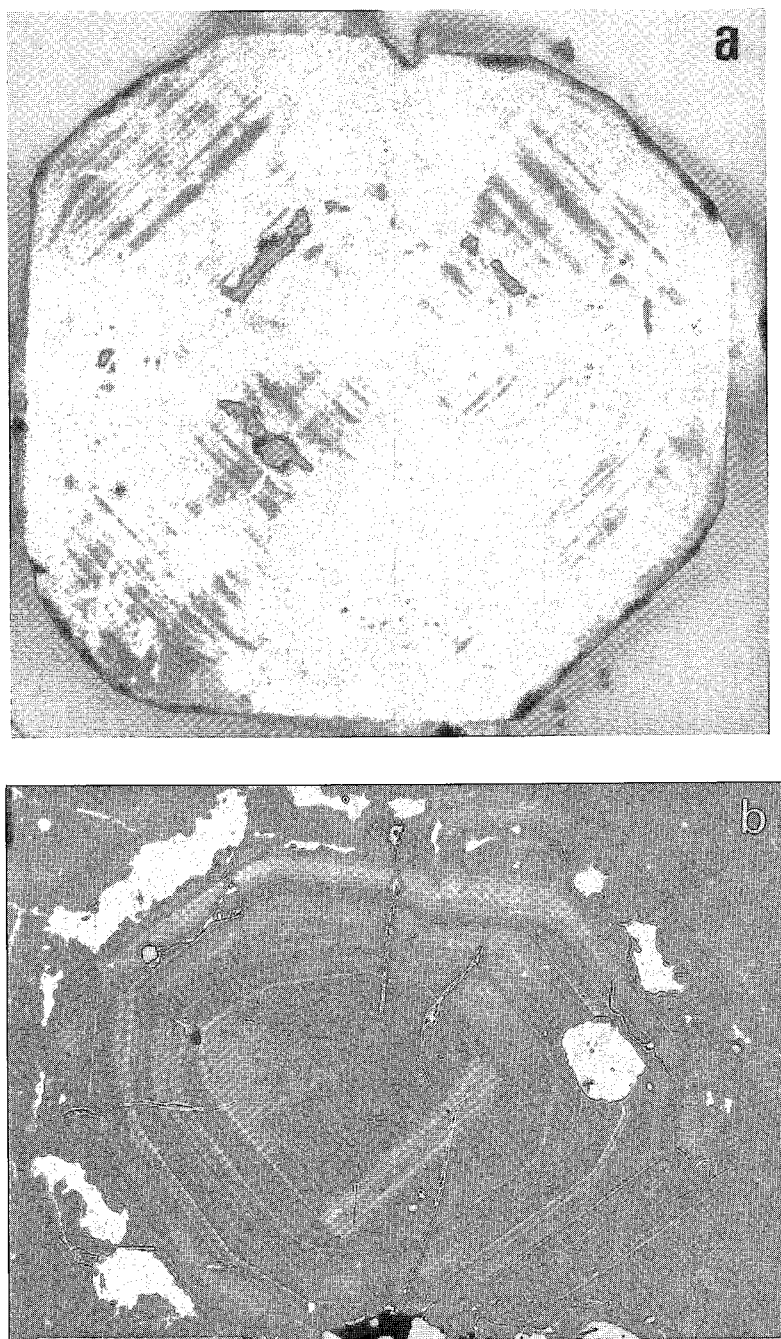
TABLE 2. UNCONSTRAINED CELL DIMENSIONS FOR V12*

	V12 core	V12 inter.	V12 rim
a (Å)	15.516(2)	15.518(2)	15.522(2)
b (Å)	15.521(1)	15.519(2)	15.548(2)
c (Å)	11.800(2)	11.810(1)	11.816(2)
α (°)	90.00(1)	89.99(1)	89.96(1)
β (°)	90.05(1)	90.05(9)	90.05(1)
γ (°)	89.97(1)	90.02(1)	90.07(1)
V (Å³)	2841.9(7)	2844.1(6)	2851.6(7)
Δ *a* (Å)	0.005	0.001	0.026

*Sample numbers are from Groat *et al.* (1992a).

FIG. 2. (a) (001) section of a normal vesuvianite (×30; V40, Monte Somma, Italy) in plane-polarized light, showing optical zoning; (b) BSE image of the core of V40, showing compositional zoning. Scale bar: 500 μm.

fringence, 2V and optical orientation; these areas tend to have straight boundaries, but do not seem to show any preferred crystallographic orientation. A high-birefringence rim and a rudimentary low-birefringence core may be present. These features are illustrated in Figure 3a for a sample from the Jeffrey mine, Quebec
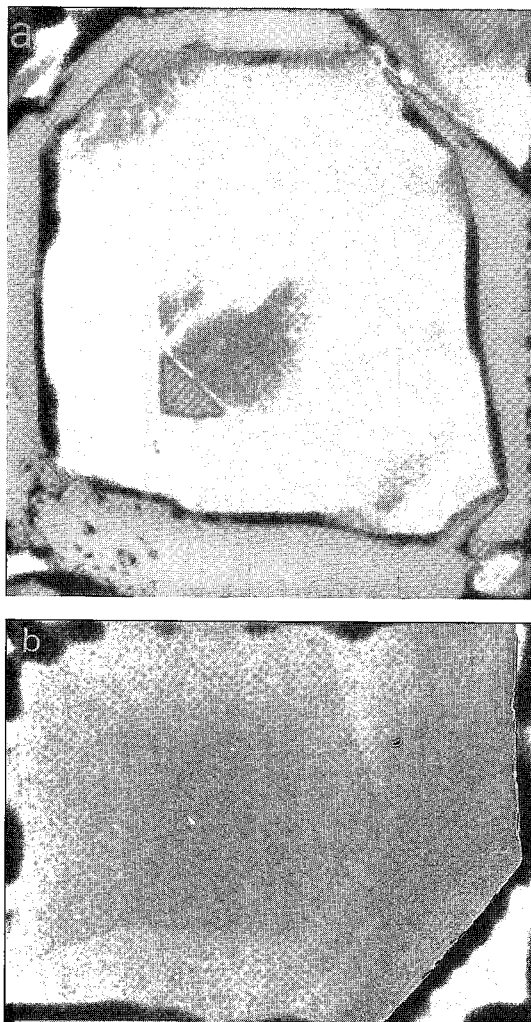
FIG. 4. Sketch of (001) section through V12, as seen in cross-polarized light.

FIG. 3. (a) (001) section (×20) of V22 (blocky vesuvianite) in cross-polarized light, showing optical zoning; (b) BSE image of one corner of V22, showing compositional zoning between the rim and the rest of the crystal. Scale bar: 500 μm.

(V22; note that samples from this locality are very variable with regard to all properties). A highly bire-fringent zone ($2V = 48°$) surrounds a blocky zone with undulose extinction and variable birefringence ($16 < 2V < 21°$). A BSE image (Fig. 3b) shows signifi-cant compositional differences between the rim and the rest of the crystal. (iii) *Sector-zoned vesuvianite:* (001) sections of these crystals show a low-birefrin-gence core and a high-birefringence rim, with addi-tional sectors or zones that vary from sample to sample; some show an intermediate-birefringence zone around the core, whereas others show distinct sectors along the [110] directions of the crystal.
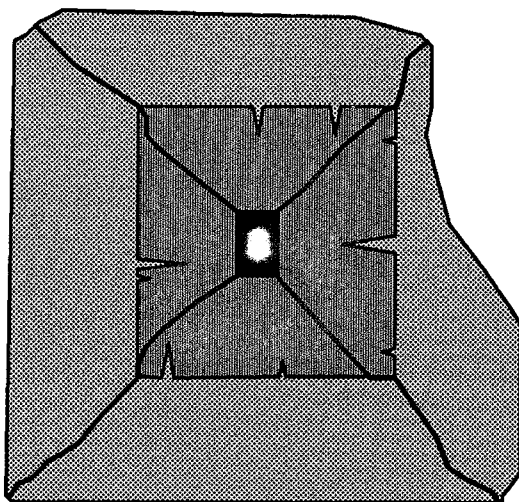
One particular type-(iii) sample from the Jeffrey mine (V12) is translucent, pale brown, and forms {100} prisms singly terminated by {101} and {001} forms. A single crystal was sectioned, and a sketch is shown in Figure 4. Each zone in the (001) section can be associated with a face of the crystal; these zones will be henceforth denoted by the corresponding face-symbol or form-symbol. The {001} sector (core) has low birefringence; $2V$ varies from 0 to 10°, and the optic axis is parallel to Z. The {101} sectors have intermediate birefringence and $2V = 36°$ with strong dispersion ($r \ll v$). The {100} sectors (rim) have high birefringence (~0.003); $2V$ is approximately equal to 60–62°. In all sectors, the optic axial plane is orient-ed orthogonal to the sector boundaries [*i.e.*, || || (010) in {101} and {100} sectors]. This was characteristic of all crystals and all samples examined. Precession photography confirmed that the principal morpho-logical form present is {100} rather than {110}.

Sample V75 from the Wilui River, former U.S.S.R., occurs as large doubly terminated crystals with promi-nent {100} and {101} and less prominent {001} and {110}, set in an extensively serpentinized matrix. Figure 5 shows part of a (001) section; the core has a cross-hatched pattern (possibly due to twinning), and the rim and {110} sectors show fine striations. The {001} sector has a low birefringence, and $2V$ varies from 0 to 10°; the {100} sectors have higher birefrin-gence, and $2V$ varies in the range 10–25°. Again, all sectors are optically positive, and V75 is an example of boron-bearing vesuvianite. BSE images indicate the presence of chemical differences between the various sectors. The sector-zoned vesuvianite V44 from Mexico closely resembles V75; both have weakly developed sector-zoning, are optically positive and
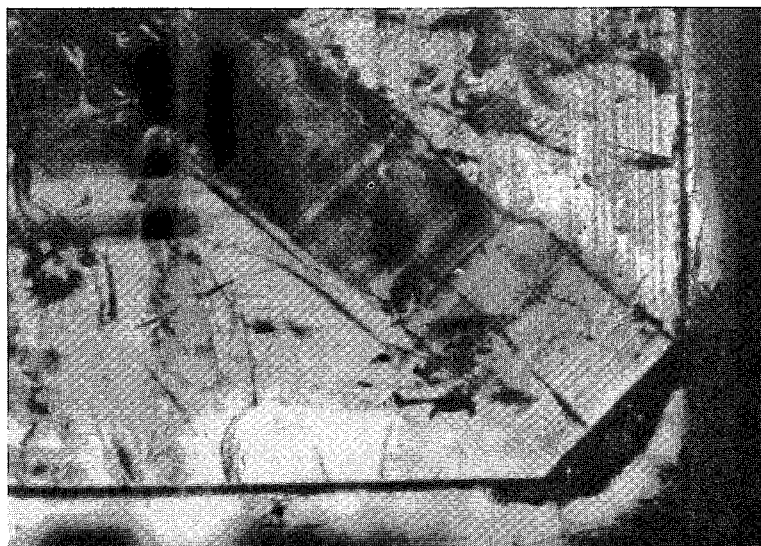
FIG. 5. Part of a (001) section of V75 in plane-polarized light ($\times$ 15), showing {100} and {110} sectors.

boron-bearing, whereas V12 and V71 have strongly developed sector-zoning, are optically negative and are boron-free.

Heating experiments. At room temperature, V12 shows sectors of different birefringence when observed down [001] in cross-polarized light; in particular, the {101} and {100} sectors show strong birefringence. With increasing temperature, the birefringence of these sectors decreases, until at ~500°C, the sectors are almost extinct. This finding suggests that the deviation from uniaxial optics decreases with increasing temperature; accurate measurements of birefringence and 2V as a function of temperature are desirable.

Precession photography

Four crystals were examined in detail. The spectacular optical zoning and large variation in 2V prompted examination of each sector in V12 from the Jeffrey mine; crystals from the {001} core, {101} intermediate, and {100} rim sectors are designated V12c, V12i and V12r, respectively. In addition, the core zone of V75 from Wilui was examined because of the presence of boron and the low content of OH.

There are two types of diffraction symmetry that we can examine by precession photography: (i) *Laue symmetry:* with regard to vesuvianite, we searched for violations of the standard 4/*mmm* symmetry on all levels. (ii) *Translational symmetry:* all elements of translational symmetry (glides, screws) give rise to "systematic absences"; in practice, the presence of such elements of symmetry imposes restrictions

on the indices of the reflections that can be observed, and "violations" of such restrictions indicate that the symmetry element is not present. P4/*nnc* has several elements of translational symmetry; these and their violating reflections are listed in Table 4. Following Allen (1985), we designate these violating reflections as being of types *a*, *b* or *c* for convenience of expression.

It should be noted that symmetry violation can be coupled between these two types. Thus violation of glide symmetry also violates the corresponding mirror symmetry of the Laue group. This connection is of some importance, as it provides supporting evidence for the absence of a glide plane. This is necessary, as the occurrence of double diffraction can give rise to additional intensity at any point in the reciprocal lattice; if the point in the reciprocal lattice has zero primary Bragg intensity because of the presence of elements of translational symmetry, this additional intensity can give the appearance of glide-violating (or screw-violating) reflections. As indicated above, all precession photographs were taken at two different precession (μ) angles, as this changes the conditions

TABLE 4. P4/*nnc* EXTINCTION CONDITIONS

Symbol	Glide Plane	Violating Conditions
a'	n glide perpendicular to *c*	hk0, h + k odd
b'	n glide perpendicular to *a*	h0l, h + l odd
		0kl, k + l odd
c'	n glide perpendicular to [110]	hhl, l odd
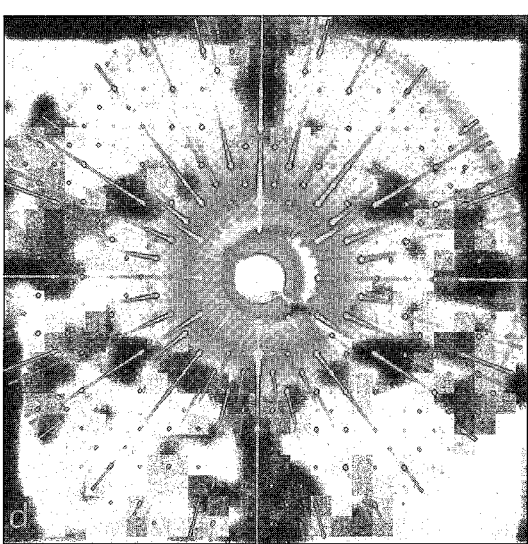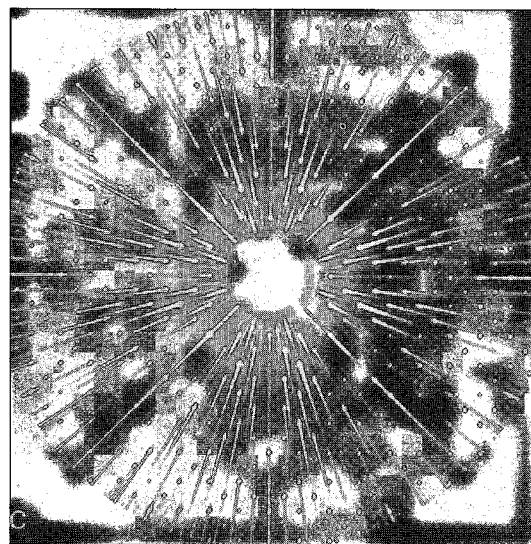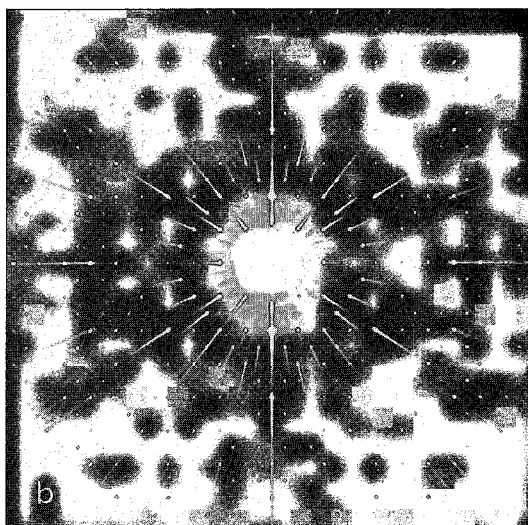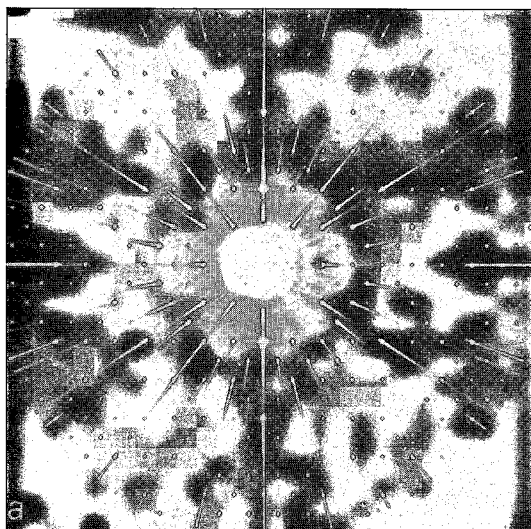
for double diffraction to occur while leaving the conditions for the occurrence of Bragg reflections unchanged. As an example of this, Figures 6a, b show two (h0l) zero-level photographs taken for V12c at a μ of 25° and 30°, respectively. Note that the prominent (702) reflection in Figure 6a is absent in Figure 6b, indicating that it is caused by double diffraction; note also that this reflection is sharper than the rest of the normal Bragg reflections, a feature that is characteristic of Renninger reflections. Reflection (702) violates all n-glide criteria in P4/nnc (Table 4), showing the importance of confirming that symmetry-violating reflections are actually true Bragg reflections, and not caused by double diffraction.

For vesuvianite V75c, there are no true violating reflections observed in any of the precession photographs. As shown in Figure 7, all reflections are sharp and round, and there is no observable streaking (diffuse intensity). Close visual inspection showed equal intensity of reflections related by 90° rotations around the Z axis, and reflections related by the horizontal and vertical mirror planes. Thus the Laue symmetry is 4/mmm, and the space-group symmetry *determined by precession photography* is P4/nnc.

In V12c (Figs. 6a, b, c), the reflections are not as sharp as those for V75c (Fig. 7), and some diffuse streaking is apparent. There is a significant number of b-type reflections (Table 5); some are quite strong [e.g., (604)], but most are relatively weak and show streaking in the a* direction. Streaking also is asso-
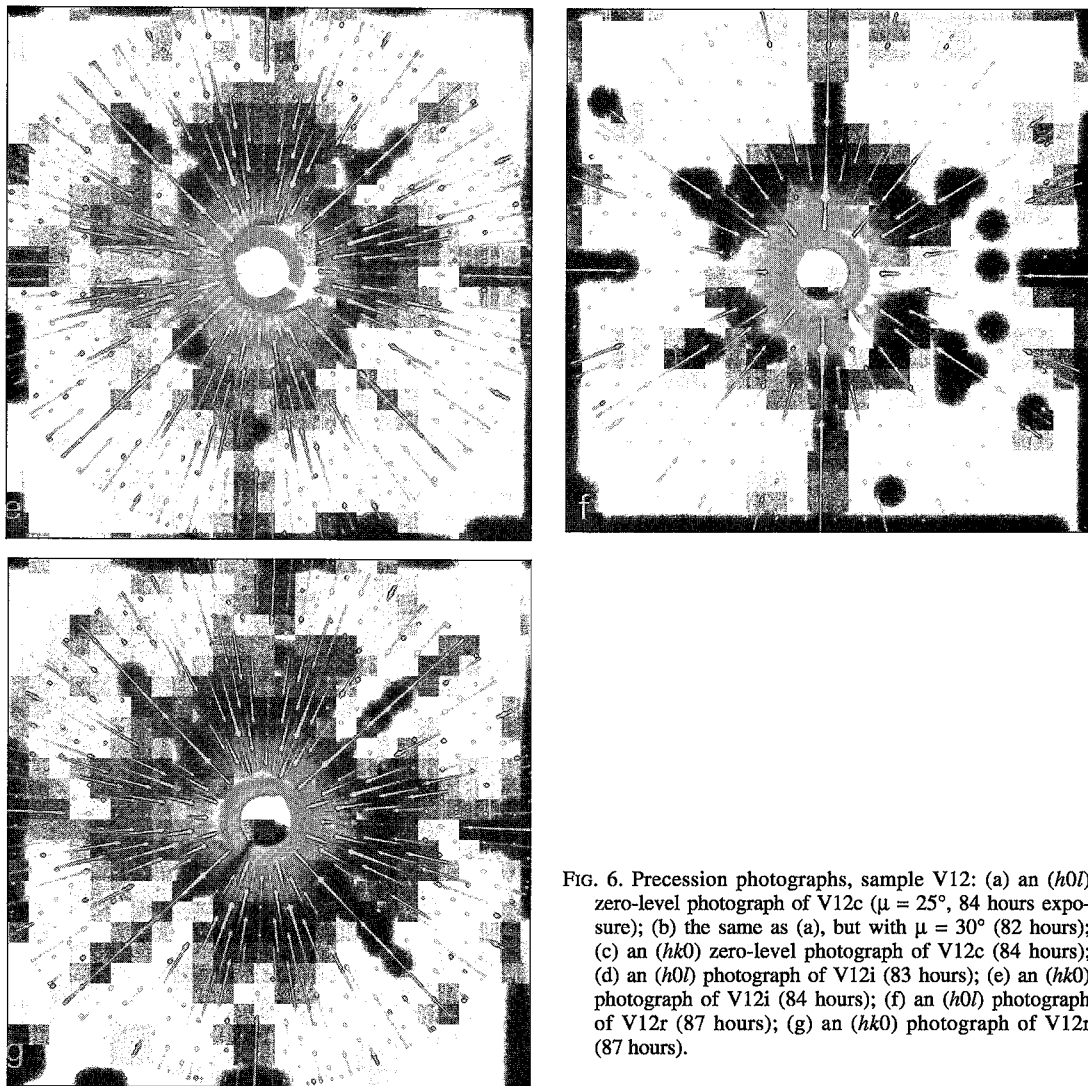
FIG. 6. Precession photographs, sample V12: (a) an (h0l) zero-level photograph of V12c ($\mu = 25°$, 84 hours exposure); (b) the same as (a), but with $\mu = 30°$ (82 hours); (c) an (hk0) zero-level photograph of V12c (84 hours); (d) an (h0l) photograph of V12i (83 hours); (e) an (hk0) photograph of V12i (84 hours); (f) an (h0l) photograph of V12r (87 hours); (g) an (hk0) photograph of V12r (87 hours).

ciated with "non-violating" reflections, and is especially noticeable on the zero-level, being prominent around (004), (008) and along (h03) and (h06) rows. The (hk0) zero-level (Fig. 6c) shows faint diagonal streaking [e.g., | | [110] around (440) and (480)]. All reflections related by 90° rotations about Z have equal intensities (as judged by eye). However, this is not the case for reflections related by vertical mirror planes; weak high-index reflections (such as 7 11 0 and 11 7 0) show notable differences in intensity, a feature that is also seen on upper-level (hk1) and (hk3) photographs. Violating reflections of type c also are observed in these upper levels, which is consistent with the loss of the diagonal vertical mirror planes in the Laue symmetry.

Corresponding precession photographs of V12i (Figs. 6d, e) show most of the features present in V12c. However, the violating reflections are considerably weaker, although the same Laue group symmetry and "space-group extinctions" are observed. A similar streaking is apparent in these photographs, although it is less prominent than in the photographs from the core {001} region.

Precession photographs for V12r are shown in Figures 6f, g. Inspection shows far more violating reflections than in V12c and V12i; these are listed in Table 5. The violating reflections are more intense and much less diffuse than is the case for analogous reflections in the core and intermediate sectors. Very little streaking is apparent in the photographs. The
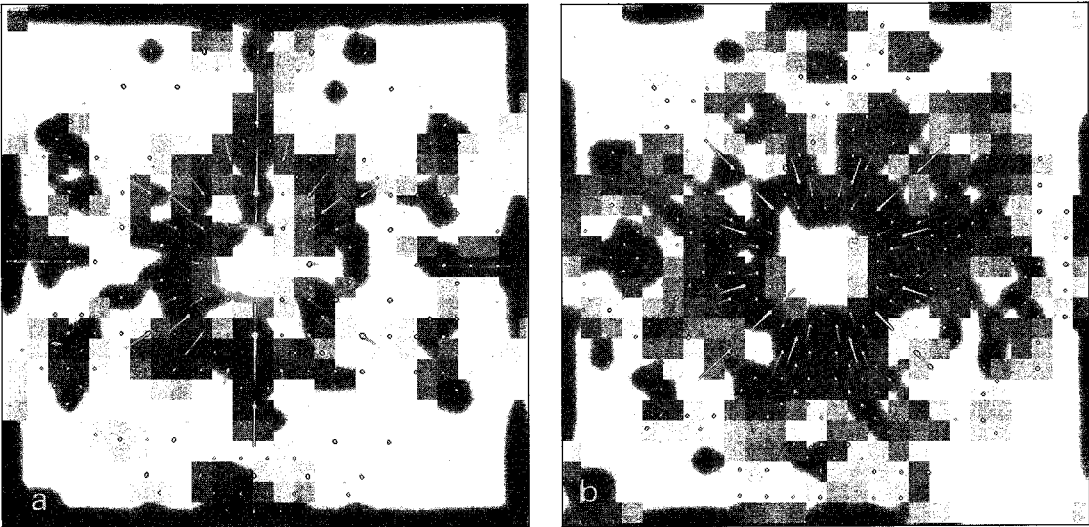
FIG. 7. Precession photographs, sample V75: (a) an (h0l) photograph (102.5 hours); (b) an (hk0) photograph (81 hours).

same Laue group symmetry is observed; the fourfold axis is retained, but there is non-equivalence across the vertical mirrors.

From the precession photography and optical results, we can make the following statements about the symmetry of vesuvianite crystals V75 and V12: (i) in V75c, no reflections seen on the precession photographs violate P4/nnc symmetry, even though 2V can range up to 10°; (ii) all sectors of V12 show b- and c-type violating reflections, together with loss of vertical mirror-plane Laue symmetry; however, no a-type reflections were observed, and the horizontal mirror

symmetry of the Laue group is retained. There is also no diffraction evidence for the loss of fourfold rotational symmetry ‖ Z, despite the fact that 2V ranges up to 62°. The precession photographs thus indicate that the *maximum* symmetry of V12 is P4/n, and show no evidence of departure from tetragonal symmetry.

Single-crystal intensity data

These data provide two types of evidence concerning the diffraction symmetry of vesuvianite: (i) systematic investigation of Laue symmetry, and (ii) complete and quantitative measurement of violating reflections.

Allen (1985) reported that a crystal of vesuvianite from Eden Mills (Vermont) shows an unequal distribution of intensities over the (hkl) set equivalent in Laue group 4/mmm, and concluded that this sample has Laue group symmetry 4/m. Table 6 shows this particular set of reflections for all four crystals (V75c, V12c, V12i, V12r) examined in detail here; only half

TABLE 5. REFLECTIONS VIOLATING EXTINCTION CONDITIONS FOR P4/nnc FROM X-RAY PRECESSION PHOTOGRAPHS (V12)

hhl	a' b' c'	hhl	a' b' c'	hhl	a' b' c'
		V12 core			
0 1 4	x	4 4 1	x	8 8 1	x
0 1 6	x	5 0 2	x	9 9 1	x
1 0 4	x	5 0 6	x	10 0 3	x
1 0 6	x	6 6 1	x	10 10 1	x
1 0 12	x	7 7 1	x	11 11 1	x
2 0 3	x	8 0 3	x	15 15 1	x
3 0 6	x				
		V12 intermediate			
1 0 1	x	2 0 3	x	5 0 2	x
1 0 4	x	2 0 5	x	6 6 1	x
1 0 6	x				
		V12 rim			
0 1 4	x	3 0 4	x	8 0 3	x
0 1 6	x	3 0 6	x	8 8 1	x
0 1 8	x	3 0 8	x	9 0 10	x
0 1 12	x	3 0 12	x	9 0 12	x
0 1 14	x	4 4 1	x	10 0 3	x
1 0 4	x	5 0 2	x	10 0 7	x
1 0 6	x	5 0 6	x	10 10 1	x
1 0 8	x	5 0 8	x	11 0 2	x
1 0 12	x	6 6 3	x	11 11 1	x
2 0 3	x	6 6 1	x	12 12 1	x

TABLE 6. INTENSITIES (cps x 10⁻³) FOR 346 AND EQUIVALENT REFLECTIONS (P4/nnc)

hkl	V75 core	V12 core	V12 inter.	V12 rim
$\bar{4}$ 3 $\bar{6}$	215(3)	499(4)	235(3)	290(3)
$\bar{4}$ 3 6	217(3)	496(4)	223(3)	293(3)
$\bar{3}$ 4 $\bar{6}$	214(3)	490(4)	228(3)	263(3)
$\bar{3}$ 4 6	219(3)	495(4)	233(3)	257(3)
3 4 $\bar{6}$	211(3)	484(4)	225(3)	298(3)
3 4 6	215(3)	476(4)	228(3)	299(3)
4 3 $\bar{6}$	216(3)	482(4)	227(3)	260(3)
4 3 6	213(3)	484(4)	223(3)	264(3)

of the reflections were measured, as the other half of the set are the Friedel equivalents. For V75c, there is no significant variation in intensity; the mean value is 215, with a dispersion of ± 4, as compared with the standard deviation of 4 for an individual intensity. Similar calculations for the various zones of V12 show significant differences in the intensities of potentially equivalent reflections. This is particularly noticeable for V12r, in which the reflections split up into two equivalent sets of mean intensities, 295(4) and 261(3), respectively; this difference of 34 can be compared with the pooled standard deviation of 4.6 to indicate that this difference is highly significant. Similar relations occur for other specific sets of reflections (*e.g.*, {124}, {126}, {133} and {137} are particularly notable in this regard), with much larger deviations than for {346}. However, for V12, they only split up into the same two sets as {346}; the 4-fold rotational symmetry is preserved for all sets of reflections examined. It should be noted that the glide-violating reflections do *not* show this same relationship; they seem to obey complete 4/*mmm* Laue symmetry. Thus for V12r, all vertical mirror planes are lost from the Laue group 4/*mmm*, resulting in 4/*m* Laue symmetry.

In the collection of the single-crystal intensity data for all four crystals, reflections systematically absent in *P4/nnc* were collected and processed in the same way as all allowed Bragg reflections; thus we measure the intensity of all potentially violating reflections. All violating reflections exceeding 5σ (based on counting statistics) are shown in Table 7. Certainly for V12c and V12r, there are many observed ostensibly violating reflections. However, these may be due to double diffraction, and it is necessary to confirm at least some of them as Bragg reflections. This may be done by monitoring the reflection intensity as the crystal is rotated about the psi vector. When the crystal is in the Bragg diffracting position, the direction orthogonal to the plane of the reflection is called the psi direction (or vector). If the crystal is rotated about the psi vector, the conditions for Bragg diffraction remain unchanged; however, the conditions for double diffraction do not remain so; consequently, reflections due to double diffraction can be detected by loss of intensity upon crystal rotation about psi. Some of the stronger violating reflections in Table 7 were examined in this fashion to confirm their validity as Bragg reflections. Figure 8 shows results of psi-scans for reflections 210 from V12i and reflections 3̄3̄3̄, 540, and 10·0̄3̄ from V12r. For reflections 210 and 540, the observed intensities scatter about zero as the crystals are rotated around psi; double diffraction is apparent as sharp spikes above background (where the doubly diffracted beam coincides

TABLE 7. REFLECTIONS VIOLATING EXTINCTION CONDITIONS FOR *P4/nnc* FROM X-RAY INTENSITY DATASETS ($F/\sigma F > 5.00$)

hhl	F/σF V12c*	F/σF V12i	F/σF V12r	a'	b'	c'	hhl	F/σF V12c	F/σF V12i	F/σF V12r	a'	b'	c'
$\overline{19}$ 0 $\bar{2}$	10.73	-	-	x			0 10 $\bar{3}$	6.00	-	10.07	x		
$\overline{10}$ 0 $\bar{3}$	-	-	10.09	x			0 10 3	5.45	-	9.46	x		
$\overline{10}$ 0 3	-	-	9.38	x			0 11 $\bar{6}$	8.45	-	-	x		
$\bar{7}$ 7 $\bar{7}$	-	-	8.71		x		0 11 2	-	-	8.68	x		
$\bar{7}$ 7 3	5.93	-	-		x		0 11 8	5.08	-	-	x		
$\bar{7}$ 7 7	5.04	-	11.20		x		0 14 11	5.70	-	-	x		
$\bar{4}$ 0 $\bar{3}$	-	-	10.65	x			1 0 $\bar{4}$	7.38	-	14.64	x		
$\bar{4}$ 0 3	-	-	9.35	x			1 0 $\bar{2}$	-	-	8.01	x		
$\bar{3}$ 3 $\bar{3}$	-	-	10.48		x		1 0 4	6.17	-	17.92	x		
$\bar{3}$ 3 3	-	-	10.79		x		1 1 11	5.03	-	-			x
$\bar{2}$ 2 $\bar{3}$	-	-	10.63		x		2 0 $\bar{5}$	-	5.02	-	x		
$\bar{2}$ 2 3	-	8.14	9.84		x		2 2 $\bar{3}$	-	-	8.56			x
$\bar{1}$ 0 $\bar{5}$	-	-	10.07	x			2 2 3	-	-	10.16			x
$\bar{1}$ 0 $\bar{4}$	6.84	-	15.20	x			3 0 $\bar{5}$	7.41	-	-	x		
$\bar{1}$ 0 4	5.19	-	14.84	x			3 3 $\bar{3}$	-	-	10.06			x
$\bar{1}$ 0 6	-	-	8.64	x			3 3 3	-	-	8.19			x
0 0 $\overline{11}$	-	-	10.86	x	x		4 0 $\bar{3}$	-	-	8.95	x		
0 0 $\bar{5}$	-	5.23	-	x	x		4 0 3	-	-	10.77	x		
0 0 11	-	-	11.44	x	x		6 6 $\bar{3}$	5.20	-	-			x
0 1 $\bar{6}$	5.03	-	-	x			7 0 10	-	6.99	-	x		
0 1 $\bar{4}$	6.20	-	16.55	x			7 7 $\bar{7}$	-	-	8.05			x
0 1 4	-	-	14.73	x			7 7 7	-	-	8.87			x
0 4 $\bar{3}$	-	-	10.50	x			10 0 $\bar{3}$	-	-	11.02	x		
0 4 3	-	-	10.28	x			10 0 3	-	-	9.72	x		
0 7 $\bar{2}$	-	9.42	-	x			11 0 $\bar{2}$	8.62	-	-	x		
0 7 6	-	5.66	-	x			19 0 2	9.77	-	-	x		

*c = core, i = intermediate zone, r = rim
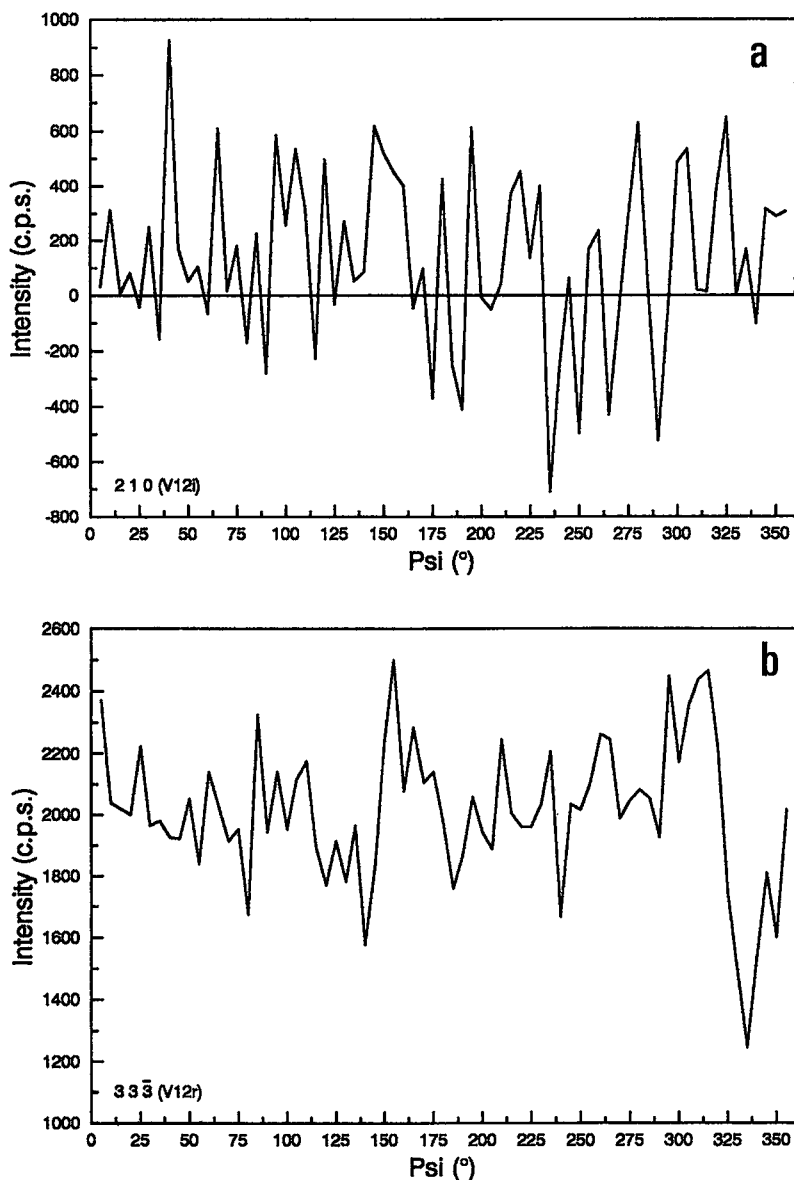
with the position of the Bragg peak) and sharp spikes below background (where the doubly diffracted beam coincides with the position of a background measurement). For reflections $33\bar{3}$ and $10 \cdot 0\bar{3}$, the observed intensities scatter about positive values (~1500 and 2000 cps, respectively); thus although double diffraction does occur at some values of psi, giving the characteristic spiky profile to the scan, these two reflections are valid Bragg reflections.

Possible space-groups

The basic structure of vesuvianite has space-group symmetry *P4/nnc*, and thus any simple structural modification of this can only occur in a space group that is a subgroup or supergroup of this basic symmetry. There are no three-dimensional space groups that are supergroups of *P4/nnc*; this limits the possible space-group symmetries to subgroups of *P4/nnc*. These may be derived from the group multiplication table for *P4/nnc* (Table 8) by systematic deletion of elements, such that the remaining elements satisfy the basic axioms of group theory and hence constitute a space group; note that as *P4/nnc* is of rank 16; derivative space-groups must have ranks of 8, 4, 2 or 1. Iteration of this procedure through all possibilities
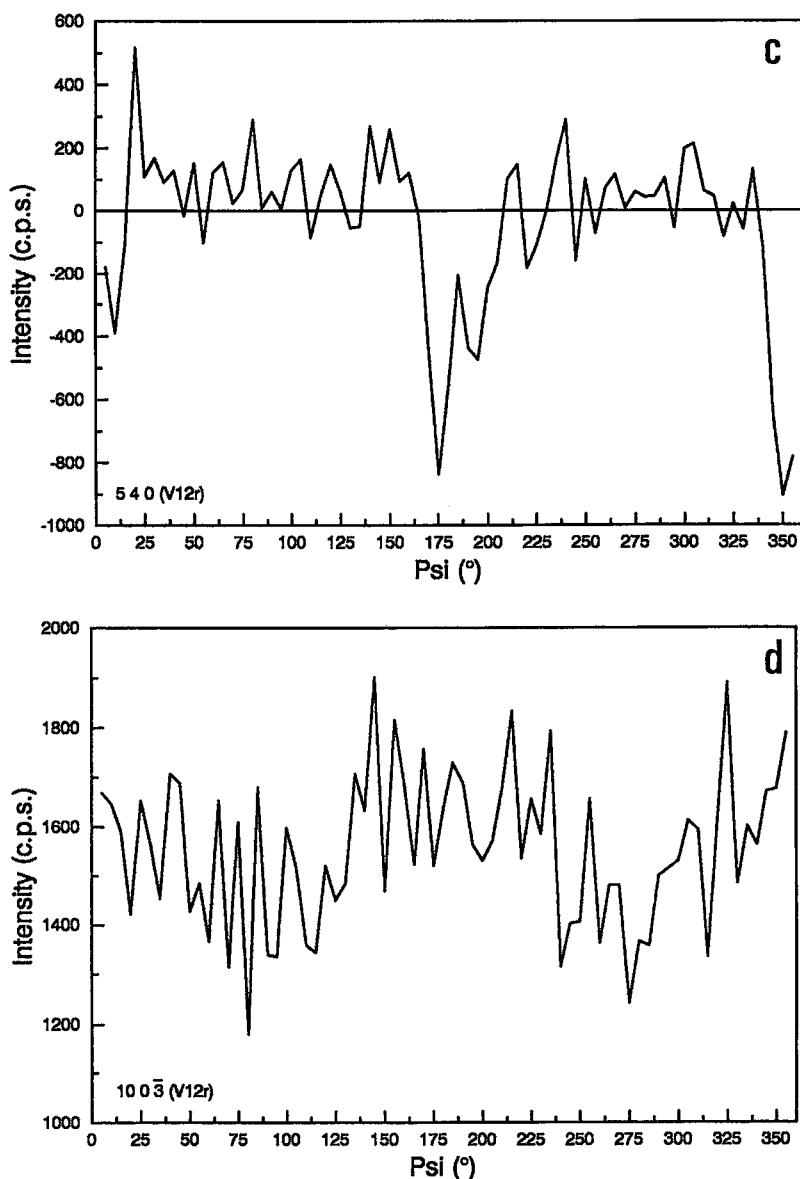
FIG. 8. Psi scans: (a) 210 from V12i, (b) 33$\overline{3}$ from V12r, (c) 540 from V12r, and (d) 10·0$\overline{3}$ from V12r.

gives the space groups of Table 9, which hence contains all possible space-group symmetries for vesuvianite structures. *Note that several space-groups suggested by previous authors are not present,* and hence such proposals cannot be correct.

High-resolution transmission electron microscopy

A (100) section of V12 was examined using high-resolution transmission electron microscopy. A hole was milled through the sample in such a way that all three sectors ({100}, {101}, and {001}) could be examined. A careful search of each sector showed no evidence of domain structure or variable intensity. However, in moving from one sector to another, it was necessary to tilt the stage in order to recenter the image of (001). Further investigation showed that in the {101} and {001} sectors, Z tilts inward (toward the center of the crystal) by as much as 3°. This agrees with optical observations.

TABLE 8. MULTIPLICATION TABLE FOR $P4/nnc$

	I	i	4^1	4^2	4^3	n^x	$\bar{4}^1$	$\bar{4}^3$	2^x	n^x	2^y	n^y	$2'$	n'	2_l	c
I	I	i	4^1	4^2	4^3	n^x	$\bar{4}^1$	$\bar{4}^3$	2^x	n^x	2^y	n^y	$2'$	n'	2_l	c
i	i	I	$\bar{4}^1$	n^x	$\bar{4}^3$	4^2	4^1	4^3	n^x	2^x	n^y	2^y	n'	$2'$	c	2_l
4^1	4^1	$\bar{4}^1$	4^2	4^3	I	$\bar{4}^3$	n^x	i	2_l	c	$2'$	n'	2^x	n^x	2^y	n^y
4^2	4^2	n^x	4^3	I	4^1	i	$\bar{4}^3$	$\bar{4}^1$	2^y	n^y	2^x	n^x	2_l	c	$2'$	n'
4^3	4^3	$\bar{4}^3$	I	4^1	4^2	$\bar{4}^1$	i	n^x	$2'$	n'	2_l	c	2^y	n^y	2^x	n^x
n^x	n^x	4^2	$\bar{4}^3$	i	$\bar{4}^1$	I	4^3	4^1	n^y	2^y	n^x	2^x	c	2_l	n'	$2'$
$\bar{4}^1$	$\bar{4}^1$	4^1	n^x	$\bar{4}^3$	i	4^3	4^2	I	c	2_l	n'	$2'$	n^x	2^x	n^y	2^y
$\bar{4}^3$	$\bar{4}^3$	4^3	i	$\bar{4}^1$	n^x	4^1	I	4^2	n'	$2'$	c	2_l	n^y	2^y	n^x	2^x
2^x	2^x	n^x	$2'$	2^y	2_l	n^y	n'	c	I	i	4^2	n^x	4^1	$\bar{4}^1$	4^3	$\bar{4}^3$
n^x	n^x	2^x	n'	n^y	c	2^y	$2'$	2_l	i	I	n^x	4^2	$\bar{4}^1$	4^1	$\bar{4}^3$	4^3
2^y	2^y	n^y	2_l	2^x	$2'$	n^x	c	n'	4^2	n^x	I	i	4^3	$\bar{4}^3$	4^1	$\bar{4}^1$
n^y	n^y	2^y	c	n^x	n'	2^x	2_l	$2'$	n^x	4^2	i	I	$\bar{4}^3$	4^3	$\bar{4}^1$	4^1
$2'$	$2'$	n'	2^y	2_l	2^x	c	n^y	n^x	4^3	$\bar{4}^3$	4^1	$\bar{4}^1$	I	i	4^2	n^x
n'	n'	$2'$	n^y	c	n^x	2_l	2^y	2^x	$\bar{4}^3$	4^3	$\bar{4}^1$	4^1	i	I	n^x	4^2
2_l	2_l	c	2^x	$2'$	2^y	n'	n^x	n^y	4^1	$\bar{4}^1$	4^3	$\bar{4}^3$	4^2	n^x	I	i
c	c	2_l	n^x	n'	n^y	$2'$	2^x	2^y	$\bar{4}^1$	4^1	$\bar{4}^3$	4^3	n^x	4^2	i	I

TABLE 9. SUBGROUPS OF $P4/nnc$

Tetragonal

$P4/nnc$	$P422$	$P4/n$
	$P4nc$	$P4$
	$P\bar{4}n2$	$P\bar{4}$
	$P\bar{4}2c$	

Orthorhombic

$Pnnn$	$Pncn^*$	$Pcnn$
$P222$	$P2_122^*$	$P22_12$
$Pnn2$	$Pnc2^*$	$Pcn2$
$Pn2n$	$Pn2n^*$	$Pc2_1n$
$P2nn$	$P2_1cn^*$	$P2nn$

Monoclinic

$P2^x/n$		
Pn		
$P2^x$†	$P2^x$	$P2^{[110]}$ $P2_1^{[110]}$

Triclinic

$P\bar{1}$
$P1$

*Principal axes at 45° to the tetragonal a axes.
†Superscripts for the monoclinic space groups indicate the orientation of the principal axis relative to the ideal tetragonal axes.

DISCUSSION

The symmetry of vesuvianite

Different crystals of vesuvianite show different degrees of deviation from $P4/nnc$ symmetry. With regard to this, the following questions are pertinent: (i) do any samples of vesuvianite have $P4/nnc$ symmetry at room temperature? (ii) do all non-tetragonal vesuvianite crystals have the same space-group symmetry? Both of these questions are difficult to answer, as very small deviations from a specific symmetry are difficult to characterize. Perhaps a more pragmatic answer to the first question is that some samples show only minor to negligible deviations from $P4/nnc$ symmetry, and the structure can be adequately described in this space group; structure refinement in a lower symmetry shows no detectable deviations from $P4/nnc$. For the second question, the same difficulties apply. What is definite is that some samples show considerable deviations from $P4/nnc$ symmetry, and the important thing is to decide on the correct (or most appropriate) space group(s) for these structures, which we refer to collectively as the low-symmetry structure.

A combination of optical and diffraction observations with the group–subgroup arguments limits the

space groups possible for low-symmetry vesuvianite to a small number of possibilities. The following observations are pertinent: (i) diffraction evidence shows that when compared to the ideal $P4/nnc$ structure, all glide-plane symmetries are violated *except* for the n-glide perpendicular to Z; (ii) optical examination shows vesuvianite to be biaxial; (iii) the optic axial plane is parallel or perpendicular to the axes of an ideal tetragonal crystal; and the (iv) possible space groups of vesuvianite must be subgroups of $P4/nnc$.

Combination of these points gives the possible space-groups of low-symmetry vesuvianite as $P2/n$ or its subgroups. For $P2/n$ symmetry, the unique axis is Z (tetragonal), and all subgroups (Pn, $P2$, $P\bar{1}$, $P1$) are possible with this orientation. However, the space group $P2$ also is possible with the unique axis along X or Y (tetragonal).

It seems worthwhile to make some fairly general remarks about the symmetry aspects of vesuvianite before specific physical and chemical details are considered. Here we have a situation where there is an obvious prototype structure (with $P4/nnc$ symmetry), and most (or all) of the structures have some type of subgroup relationship to this prototype. For the present, we allow the possibility that individual structures of vesuvianite might adopt different space-group symmetries, depending on details of chemistry or history of crystallization and equilibration. This strongly suggests that there is a continuous second-order phase transition between a (high-temperature) $P4/nnc$ structure and a lower-symmetry modification. Such situations are best considered within the framework of Landau theory (Tolédano & Tolédano 1980, Salje 1990).

Landau theory

The basic ideas of this theory are fairly simple. For a continuous phase-transition, the difference between the high-symmetry phase and the low-symmetry phase is zero at the transition. As conditions change away from the transition into the field of stability of the low-symmetry phase, the difference between the high-symmetry phase and the low-symmetry phase increases. If we normalize the difference such that its possible values are in the range 0–1, this difference is called the *order parameter;* note that we have not yet specified the physical nature of the order parameter. In a continuous phase-transition, the order parameter changes continuously from zero to non-zero values, and these non-zero values are small close to the phase transition. We can express the free energy of the system in terms of the free energy of the part corresponding to the high-symmetry phase plus the free energy of the distortions from the high-symmetry phase, that is, the order parameter. As the order parameter is small, we can expand the free energy as a Taylor series in terms of the order parameter. There are

various constraints imposed by symmetry on the coefficients of this expansion, and useful expressions for the free energy thermodynamic potential can be derived. Thus the physical idea that underlies this type of treatment is quite straightforward, although the algebraic aspects of a quantitative treatment can be rather complicated. This approach has been used by Salje and coworkers (Salje 1985, 1987, Salje *et al.* 1985, Redfern & Salje 1987) and by Hatch and coworkers (Hatch *et al.* 1987, Hatch & Ghose 1989a, b, Hatch & Griffen 1989) for the analysis of phase transitions in some minerals.

Application to vesuvianite

The limited information on the temperature dependence of the optical data shows the (spontaneous) birefringence down [001] to decrease with increasing temperature. This finding, together with the symmetry relationships in vesuvianite, suggest a continuous transition between a high-symmetry phase and a low-symmetry phase, from a high-temperature tetragonal (uniaxial) structure to a low-temperature (biaxial) structure. There may, in fact, be more than one transition in this system, as the high symmetry of the parent structure could allow a series of continuous transitions with decreasing temperature. Such a possibility can only be examined by detailed quantitative measurements of order parameter(s) as a function of temperature. At present, it is sufficient to identify the presence of a transition, and consider which of the unusual features of vesuvianite are a result of this transition.

In a $P4/nnc \rightarrow P2/n$ transition, the translational symmetry remains unchanged, and the critical point of the Brillouin zone is the origin. Thus the primary order-parameter must transform under a Γ point (zonecenter) representation of $P4/nnc$. Inspection of Table 1 of Stokes & Hatch (1988) shows that the active orderparameter must transform according to the one-dimensional representation Γ^{5+} of $P4/nnc$. This is a pure ferroelastic transition (Aizu 1969, Tolédano 1979), and both Landau and Lifshitz frequencies are zero, as required for a continuous transition. Hence the basis functions of the active irreducible representation transform as the components of the spontaneous strain. Schlenker *et al.* (1978) gave the generalized Lagrangian strain tensor components. Using the standard axes of vesuvianite, the components of the spontaneous strain are:

$$e_{11} = (a_t - a_m)/a_t, \; e_{22} = (a_t - b_m)/a_t, \; e_{33} = (c_t - c_m)/c_t \tag{1}$$

where the subscripts denote the symmetry of the structure. Assuming that $(a_m + c_m)/2 = a_t$ and $c_t = c_m$, we may calculate the spontaneous strain from the metrically unconstrained cell-dimensions of the vesuvianite samples of Groat *et al.* (1992a). This correlates strongly with the $2V$ values measured for these crys-
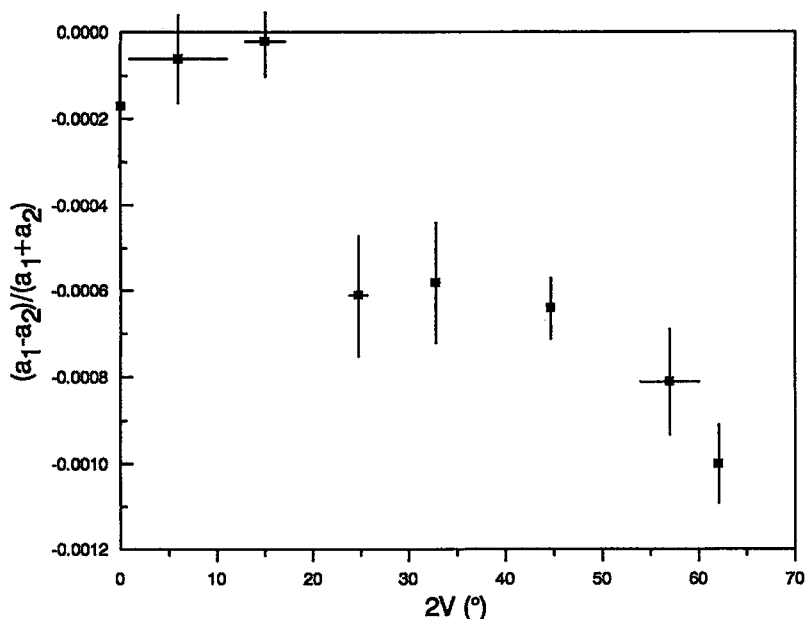
FIG. 9. Variation of spontaneous strain with optic axial angle (2V) for selected crystals of vesuvianite.

tals (Fig. 9), and also should correlate with the spontaneous birefringence.

The components of the spontaneous strain transform as the order parameter for the representation Γ^{5+}, and hence the spontaneous strain could drive the transition. However, all suggestions as to the possible symmetry-lowering mechanism in vesuvianite have involved cation ordering; we will consider this next.

Ordering of channel cations as an order parameter

There have been several suggestions that lowering of symmetry in vesuvianite primarily involves ordering of cations over the channel sites $X(4)A + X(4)B$ and $Y(1)A + Y(1)B$ (Table 10). However, the order parameters associated with such mechanisms do not transform as the Γ^{5+} irreducible representation of $P4/nnc$, and hence cannot drive a (ferroelastic) $P4/nnc \rightarrow P2/n$ phase transition. They can drive a ferroic transition, $P4/nnc \rightarrow P4/n$, but the basic problem in vesuvianite involves breaking of tetragonal symmetry, and such channel ordering cannot be the cause of this (unless the lower symmetry is $P2$ rather than $P2/n$, in which case ordering over quartets of channel sites (Table 10) would occur and could drive the transition).

Ordering of channel cations and diffraction symmetry

There have been several refinements of the structure of vesuvianite in space group $P4/n$, and these

have shown significant ordering of cations over sites that are equivalent in $P4/nnc$. Specifically, the channel sites [labeled Ca(4)A and Ca(4)B, and M(3)A and M(3)B by Giuseppetti & Mazzi (1983)] have split into two sets of two equivalent sites, rather than one set of four equivalent sites in the $P4/nnc$ structure. It is instructive to examine the expression for the structure factor in $P4/n$, and see the effect of ordering on the diffraction characteristics. Using standard terminology (International Tables for X-ray Crystallography,

TABLE 10. CHANNEL SITES AS A FUNCTION OF SYMMETRY

P4/nnc	P4/n	P2/n, Pn, P$\bar{1}$	P2, P1
X(4)	X(4)A	X(4)A	X(4)A'
			X(4)A"
	X(4)B	X(4)B	X(4)B'
			X(4)B"
Y(1)	Y(1)A	Y(1)A	Y(1)A'
			Y(1)A"
	Y(1)B	Y(1)B	Y(1)B'
			Y(1)B"

1974), the structure factor may be written as

$$A = 8\cos\pi([h-k]x + [h+k]y - h/2)\cos\pi([h+k]x - [h-k]y - k/2)\cos2\pi(lz + [h+k]/4) \quad (2)$$

For the $Y(1)A$ and $Y(1)B$ sites, $x = y = 1/4$, and equation (2) reduces to

$$a = 8\cos2\pi(h/4+k/4+lz) \quad (3)$$

As this is symmetrical in h and k, $A_{hkl} = A_{khl}$ for $x = y = 1/4$, and ordering over $Y(1)A$ (1/4, 1/4, z) and $Y(1)B$ (1/4, 1/4, z') does not break $4/mmm$ Laue symmetry. Thus the deviations from $4/mmm$ Laue symmetry noted above must be caused by other structural factors than ordering over the $Y(1)A$ and $Y(1)B$ sites. On the other hand, such ordering can produce intensity for reflections of the type $h0l$, $h + l = 2n + 1$, and hence the occurrence of vertical-glide-violating reflections could be due to ordering over $Y(1)A$ and $Y(1)B$.

There are two important points that result from the above considerations: (i) the argument generalizes to all channel sites, and hence channel ordering of any kind is not sufficient to describe a change in symmetry from $P4/nnc$ to $P4/n$. There must be significant changes in order or atomic positions at sites lying off the channels through the structure, possibly occurring as relaxation in response to ordering of channel cations. Also, the only diffraction information on order of cations in the channels lies in the glide-violating reflections. (ii) Ordering of channel cations of this type cannot account for the deviations from tetragonal symmetry (as shown above when considering the group-theory aspects of a $P4/nnc \rightarrow P2/n$ transition). In principle, ordering of channel cations such that $Y(1)$ splits into four distinct sites could drive a $P4/nnc \rightarrow P2$ transition, and it is perhaps significant that Allen & Burnham (1992) reported positive SHG (Second Harmonic Generation) signals from samples of vesuvianite showing strong glide-violating reflections, suggesting non-centrosymmetric space-group symmetry.

As noted above, ordering of cations over pairs of channel sites cannot drive a $P4/nnc \rightarrow P2/n$ transition. However, such ordering does contribute to the intensity of reflections of types a, b and c (Table 4). Inspection of Tables 5 and 7 shows the relationship between the intensities of the violating reflections and the deviation from tetragonal symmetry, as measured by $2V$ in the {001} ($2V = 0$–10°), {101} ($2V = 36°$) and {100} ($2V = 61°$) zones of sample V12. Although the violating reflections are strongest for the {100} zone, where $2V$ is largest, the violating reflections are weakest for the {101} zone, where $2V$ is still quite large (36°), and intermediate between these two for the {001} zone, where $2V$ is small. Thus there is not a 1:1 correlation between the intensity of the violating reflections and the deviation from tetragonal symmetry as measured by the observed $2V$ values. This throws some doubt on the presence of a $P4/nnc \rightarrow P2$

transition driven by ordering of cations over quartets of channel sites, as in that case, one might expect a direct relationship between the intensities of the violating reflections and $2V$. This also suggests that we will not identify the principal order-parameter until there has been an adequate structural refinement of a monoclinic vesuvianite (work in progress).

Twinning in vesuvianite

Many investigators have proposed that twinning occurs in vesuvianite, both to account for the appearance of some samples in transmitted light, and to account for its unusual physical and diffraction properties. We regard it as possible that many vesuvianite samples may be twinned. However, this is not the *reason* why vesuvianite deviates from tetragonal symmetry.

Twinning of the kind usually proposed for vesuvianite (*e.g.*, by reflection across a mirror | | {110}) will *increase* the apparent symmetry for most physical processes such as transmission of light or diffraction of X rays, provided that the scale of the twinning is fine relative to the energetic or spatial resolution of the process. Hence twinning will tend to *reduce* the optical or diffraction "anomalies" of a mineral and cannot normally contribute to such features. Thus although twinning may be present in vesuvianite, it cannot be a causative factor for the "anomalous" features of this mineral.

Antiphase domains

Several samples of vesuvianite have been refined in the space-group $P4/n$, with the resulting patterns of order among channel cations distinct from those expected in $P4/nnc$ symmetry. In the transition $P4/nnc \rightarrow P4/n$, there are two possible origins of the $P4/n$ cell relative to the parent $P4/nnc$ cell: (0,0,0) and (1/2,0,1/2). Thence there is the possibility of the development of antiphase domains of $P4/n$ structure with a relative displacement of (0,0,1/2).

Veblen & Weichmann (1991) have recently shown that a vesuvianite crystal from Crestmore, California, is made up of domains 10–50 nm wide elongate parallel to [001]. This particular specimen shows selected-area electron-diffraction patterns consistent with $P4/n$ symmetry, but is weakly optically biaxial; Veblen & Weichmann (1991) suggested that the true symmetry of this vesuvianite is $P2/n$ or lower. On the other hand, our HRTEM examination of vesuvianite V12 from the Jeffrey mine, Quebec, shows no sign of any antiphase domains. In particular, the {100} sector shows strong deviation from tetragonal symmetry and uniaxial optical behavior ($2V \approx 60°$), in line with the absence of domain structure (as the twin relationship between different domains will tend to average out deviations from tetragonal behavior in macroscopic or

long-range properties). This is in line with the idea of a high-temperature (>500°C) phase transition, where crystals forming above the transition will invert to the lower symmetry through the transition, forming finely twinned domains (*cf.* Veblen & Weichmann 1991), whereas crystals forming below the transition will be untwinned and will have the lower-symmetry structural arrangement over the long range.

The origin of sector zoning

Sector zoning is observed in many minerals, and has been explained as a result of differences in composition or degree of order that relate to differential interaction of components with different crystal-growth faces of a mineral. This mechanism can be invoked here to rationalize sector-zoned vesuvianite, as our chemical data show small but significant compositional differences between sectors.

As yet, there has not been a successful refinement of the structure of a non-tetragonal vesuvianite (currently under investigation by us), and thus the complete details of the physical mechanism associated with the (tetragonal) symmetry-breaking transition are not known. In terms of crystal growth, the attitude of the structure with respect to the growing faces of the crystal is of obvious importance in terms of the character of the order parameter that drives the transition.

Temperature range of crystallization

The presence of a (continuous) phase transition accounts for many (but not all) of the physical features observed in vesuvianite, the key aspect being the relationship of the temperature of transition to the temperature interval of crystallization of the specific sample. We can recognize three situations: (i) The temperature interval of crystallization is above the temperature of the transition. In this case, the vesuvianite crystallizes with $P4/nnc$ symmetry. On cooling, it passes through the transition and inverts to a lower symmetry, which produces fine-scale twinning. This produces the "normal" vesuvianite with uniform extinction and small ($\leq 5°$) $2V$. The fact that $2V$ does not equal zero indicates that the true symmetry is not tetragonal (*i.e.*, the crystal is not uniaxial), but the fine-scale twinning serves to simulate (pseudo-)tetragonal optical behavior. Such a twinned structure has been observed by Veblen & Weichmann (1991) in vesuvianite from Crestmore (California) that formed close to a contact with a quartz monzonite (*i.e.*, at a relatively high temperature). (ii) The temperature of crystallization is completely below the temperature of the transition. In this case, vesuvianite crystallizes with non-tetragonal symmetry, and the complexities that are observed must be due to crystal growth; this leads to sector-zoned vesuvianite. (iii) The temperature

of crystallization overlaps the temperature of the transition. In this case, vesuvianite initially crystallizes with $P4/nnc$ symmetry as in case (i). However, as the temperature falls through that of the transition, a lower-symmetry arrangement begins to crystallize, and the initial $P4/nnc$ structure inverts to the lower form with a polysynthetically twinned arrangement. This process produces a pseudo-tetragonal core with an overgrowth of strongly biaxial vesuvianite.

CONCLUSIONS

(i) Optical examination shows virtually all vesuvianite samples to be biaxial, with $2V$ varying in the range 0–62°.
(ii) X-ray data show no discernable deviation from tetragonal symmetry.
(iii) If compared to the ideal $P4/nnc$ structure, all glide-plane symmetries are violated *except* for the n-glide perpendicular to Z.
(iv) Sector-zoned vesuvianite shows compositional and optical ($2V$) differences between sectors.
(v) The optic axial plane is parallel or perpendicular to the axes of an ideal tetragonal crystal; this discounts several orthorhombic and monoclinic subgroups, with principal axes at 45° to the ideal tetragonal axes.
(vi) Optical and diffraction data indicate that vesuvianite has $P2/n$ or Pn space-group symmetry.
(vii) We suggest that vesuvianite undergoes a ferroelastic phase-transition at high temperatures (>500°C) from a $P4/nnc$ structure to a $P2/n$ or Pn structure.
(viii) Ordering of channel cations over nonequivalent pairs of $Y(1)$ and $X(4)$ sites cannot be the order parameter that drives the $P4/nnc \to P2/n$ transition, as it does not transform as the active irreducible representation of this transition.
(ix) We propose that the different optical types of vesuvianite arise from different relationships between the temperature range of crystallization and the temperature of the ferroelastic phase-transition.

REFERENCES

AIZU, K. (1969): Possible species of "ferroelastic" crystals and of simultaneously ferroelectric and ferroelastic crystals. *J. Phys. Soc. Japan* **27**, 387–396.

ALLEN, F.M. (1985): *Structural and Chemical Variations in Vesuvianite*. Ph.D. thesis, Harvard University, Cambridge, Massachusetts.

—— & BURNHAM, C.W. (1983a): Structure refinement of an iron-poor vesuvianite. *Trans. Am. Geophys. Union* **64**, 353 (abstr.).

—— & —— (1983b): Cation ordering in low-symmetry vesuvianites. *Geol. Soc. Am., Abstr. Programs* **15**, 513.

—— & —— (1992): A comprehensive structure model for vesuvianite: symmetry variations and crystal growth. *Can. Mineral.* **30**, 1-18.

AREM, J.E. (1973): Idocrase (vesuvianite) – a 250-year puzzle. *Mineral. Rec.* **4**, 164-174.

—— & BURNHAM, C.W. (1969): Structural variations in idocrase. *Am. Mineral.* **54**, 1546-1550.

BLOSS, F.D. (1961): *An Introduction to the Methods of Optical Crystallography*. Holt, Rinehart & Winston, New York.

—— (1981): *The Spindle Stage: Principles and Practice*. Cambridge University Press, New York.

FITZGERALD, S., LEAVENS, P.B., RHEINGOLD, A.L. & NELEN, J.A. (1987): Crystal structure of a REE-bearing vesuvianite from San Benito County, California. *Am. Mineral.* **72**, 625-628.

——, RHEINGOLD, A.L. & LEAVENS, P.B. (1986): Crystal structure of a non-*P4/nnc* vesuvianite from Asbestos, Quebec. *Am. Mineral.* **71**, 1483-1488.

GIUSEPPETTI, G. & MAZZI, F. (1983): The crystal structure of a vesuvianite with *P4/n* symmetry. *Tschermaks Mineral. Petrogr. Mitt.* **31**, 277-288.

GROAT, L.A., HAWTHORNE, F.C. & ERCIT, T.S. (1992a): The chemistry of vesuvianite. *Can. Mineral.* **30**, 19-48.

——, —— & —— (1992b): The role of fluorine in vesuvianite: a crystal-structure study. *Can. Mineral.* **30**, 1065-1075.

HATCH, D.M. & GHOSE, S. (1989a): A dynamical model for the $I\bar{1} - P\bar{1}$ phase transition in anorthite, $CaAl_2Si_2O_8$. II. Order parameter treatment. *Phys. Chem. Miner.* **16**, 614-620.

—— & —— (1989b): Symmetry analysis of the phase transition and twinning in $MgSiO_3$ garnet: implications to mantle mineralogy. *Am. Mineral.* **74**, 1221-1224.

—— & GRIFFEN, D.T. (1989): Phase transitions in the grandite garnets. *Am. Mineral.* **74**, 151-159.

——, STOKES, H.T. & PUTNAM, R.M. (1987): Symmetry analysis of the microstructure and phase transitions of a crystallographic space-group: applications. *Phys. Rev.* **B35**, 4935-4942.

INTERNATIONAL TABLES FOR X-RAY CRYSTALLOGRAPHY, VOL. **IV** (1974): Kynoch Press, Birmingham, England.

KHOTINA, M.I. (1968): The chemical composition of the vesuvianite with zonal and sectorial structure from the Norilsk district. *Zap. Vses. Mineral. Obshchest.*, 312-630.

OFTEDAL, I. (1964): Contributions to the mineralogy of Norway. **29**. Vesuvianite as a host mineral for boron. *Nor. Geol. Tidsskr.* **44**, 377-383.

REDFERN, S.A.T. & SALJE, E. (1987): Thermodynamics of plagioclase. II. Temperature evolution of the spontaneous strain at the $I\bar{1}-P\bar{1}$ phase transition in anorthite. *Phys. Chem. Miner.* **14**, 189-195.

SALJE, E.K.H. (1985): Thermodynamics of sodium feldspar. I. Order parameter treatment and strain induced coupling effects. *Phys. Chem. Miner.* **12**, 93-98.

—— (1987): Thermodynamics of plagioclase. I. Theory of the $I\bar{1}-P\bar{1}$ phase transition in anorthite and Ca-rich plagioclase. *Phys. Chem. Miner.* **14**, 181-188.

—— (1990): *Phase Transitions in Ferroelastic and Co-elastic Crystals: an Introduction for Mineralogists, Material Scientists, and Physicists*. Cambridge University Press, Cambridge, U.K.

——, KUSCHOLKE, B., WRUCK, B. & KROLL, H. (1985): Thermodynamics of sodium feldspar. II. Experimental results and numerical calculations. *Phys. Chem. Miner.* **12**, 99-107.

SAPOUNTZIS, E.S. & KATAGAS, C. (1980): Idocrase (vesuvianite) from the Kozani area (north Greece). *Neues Jahrb. Mineral., Monatsh.*, 461-468.

SCHLENKER, J.L., GIBBS, G.V. & BOISEN, M.B., JR. (1978): Strain-tensor components expressed in terms of lattice parameters. *Acta Crystallogr.* **A34**, 52-54.

SERDYUCHENKO, D.P., GUBAYDULIN, F.G., PAVLOV, V.A. & SUNDAKOVA, I.YA. (1968): Idocrases from skarns in central Asia and their chemical composition. *Dokl. Akad. Nauk SSSR, Ser. Geol.* **180**, 135-137 (in Russ.).

STOKES, H.T. & HATCH, D.M. (1988): *Isotropy Subgroups of the 230 Crystallographic space-groups*. World Scientific, Singapore.

TOLÉDANO, J.C. (1979): Symmetry-determined phenomena at crystalline phase transitions. *J. Solid State Chem.* **27**, 41-49.

—— & TOLÉDANO, P. (1980): *The Landau Theory of Phase Transitions*. World Scientific, Singapore.

VEBLEN, D.R. & WEICHMANN, M.J. (1991): Domain structure of a low-symmetry vesuvianite from Crestmore, California. *Am. Mineral.* **76**, 397-404.

WARREN, B.E. & MODELL, D.I. (1931): The structure of vesuvianite $Ca_{10}Al_4(Mg,Fe)_2Si_9O_{34}(OH)_4$. *Z. Kristallogr.* **78**, 422-432.